Longitudinal Chromatic Aberration of the human eye in the visible and near infrared from wavefront sensing, double-pass and psychophysics

Maria Vinas,* Carlos Dorronsoro, Daniel Cortes, Daniel Pascual, and Susana Marcos

Instituto de Óptica, Consejo Superior de Investigaciones Científicas (CSIC), Madrid, Spain
*maria.vinas@io.cfmac@csic.es

Abstract: Longitudinal Chromatic Aberration (LCA) influences the optical quality of the eye. However, the reported LCA varies across studies, likely associated to differences in the measurement techniques. We present LCA measured in subjects using wavefront sensing, double-pass retinal images, and psychophysical methods with a custom-developed polychromatic Adaptive Optics system in a wide spectral range (450-950 nm), with control of subjects' natural aberrations. LCA measured psychophysically was significantly higher than that from reflectometric techniques (1.51 D vs 1.00 D in the 488-700 nm range). Ours results indicate that the presence of natural aberrations is not the cause for the discrepancies across techniques.

OCIS codes: (260.0260) Physical optics; (330.0330) Vision, color, and visual optics; (330.4875) Optics of physiological systems; (330.5370) Psychophysics; (220.1010) Aberrations (global); (220.1080) Active or adaptive optics.

References and links

1. L. N. Thibos, A. Bradley, and X. X. Zhang, "Effect of ocular chromatic aberration on monocular visual performance," Optom Vis Sci **68**, 599-607 (1991).
2. K. Graef and F. Schaeffel, "Control of accommodation by longitudinal chromatic aberration and blue cones," J Vis **12**, 14 (2012).
3. W. N. Charman, *Optics of the Human Eye*, Visual Optics and Instrumentation (CRC Press, 1991).
4. R. E. Bedford and G. Wyszecki, "Axial chromatic aberration of the human eye," J. Opt. Soc. Am. **47**, 564-565 (1957).
5. P. A. Howarth, "The lateral chromatic aberration of the eye," Ophthalmic. Physiol. Opt. **4**, 223-226 (1984).
6. M. Rynders, B. Lidkea, W. Chisholm, and L. N. Thibos, "Statistical distribution of foveal transverse chromatic aberration, pupil centration, and angle psi in a population of young adult eyes," J. Opt. Soc. Am. A. **12**, 2348-2357 (1995).
7. L. N. Thibos, A. Bradley, D. L. Still, X. Zhang, and P. A. Howarth, "Theory and measurement of ocular chromatic aberration," Vision Res. **30**, 33-49 (1990).
8. S. Marcos, S. A. Burns, P. M. Prieto, R. Navarro, and B. Baraibar, "Investigating sources of variability of monochromatic and transverse chromatic aberrations across eyes," Vision Res. **41**, 3861-3871 (2001).
9. J. S. McLellan, S. Marcos, P. M. Prieto, and S. A. Burns, "Imperfect optics may be the eye's defence against chromatic blur," Nature **417**, 174-176 (2002).
10. E. J. Fernandez, A. Unterhuber, B. Povazay, B. Hermann, P. Artal, and W. Drexler, "Chromatic aberration correction of the human eye for retinal imaging in the near infrared," Opt. Express **14**, 6213-6225 (2006).

11. P. A. Howarth and A. Bradley, "The longitudinal chromatic aberration of the human eye, and its correction," Vision Res. **26**, 361-366 (1986).
12. X. Zhang, L. N. Thibos, and A. Bradley, "Wavelength-dependent magnification and polychromatic image quality in eyes corrected for longitudinal chromatic aberration," Optom. Vis. Sci **74**, 563-569 (1997).
13. T. Young, "An Account of Some Cases of the Production of Colours, not Hitherto Described," Philosophical Transactions of the Royal Society of London **92**, 387-397 (1802).
14. H. von Helmholtz, *Treatise on Physiological Optics (1866),* translation from third German edition (1909) ed., The classics of Ophthalmology library (University of Pennsylvania, 2001).
15. M. C. Rynders, R. Navarro, and M. A. Losada, "Objective measurement of the off-axis longitudinal chromatic aberration in the human eye," Vision Res. **38**, 513-522 (1998).
16. C. Ware, "Human axial chromatic aberration found not to decline with age," Graefes Arch. Clin. Exp. Ophthalmol **218**, 39-41 (1982).
17. P. A. Howarth, X. X. Zhang, A. Bradley, D. L. Still, and L. N. Thibos, "Does the chromatic aberration of the eye vary with age?," J. Opt. Soc. Am. A **5**, 2087-2092 (1988).
18. M. Millodot, "The influence of age on the chromatic aberration of the eye," Albrecht Von Graefes Arch. Klin. Exp. Ophthalmol. **198**, 235-243 (1976).
19. J. A. Mordi and W. K. Adrian, "Influence of age on chromatic aberration of the human eye," Am. J. Optom. Physiol. Opt. **62**, 864-869 (1985).
20. G. Wald and D. R. Griffin, "The change in refractive power of the human eye in dim and bright light," J. Opt. Soc. Am. **37**, 321-336 (1947).
21. B. Gilmartin and R. E. Hogan, "The magnitude of longitudinal chromatic aberration of the human eye between 458 and 633 nm," Vision Res. **25**, 1747-1753 (1985).
22. S. Marcos, S. A. Burns, E. Moreno-Barriusop, and R. Navarro, "A new approach to the study of ocular chromatic aberrations," Vision Res. **39**, 4309-4323 (1999).
23. D. A. Atchison and G. Smith, *Optics of the human eye* (Butterworth Heinemann, 2000), Vol. 17.
24. L. N. Thibos, M. Ye, X. Zhang, and A. Bradley, "The chromatic eye: a new reduced-eye model of ocular chromatic aberration in humans," Appl. Opt. **31**, 3594-3600 (1992).
25. W. N. Charman and J. A. Jennings, "Objective measurements of the longitudinal chromatic aberration of the human eye," Vision Res. **16**, 999-1005 (1976).
26. L. Llorente, L. Diaz-Santana, D. Lara-Saucedo, and S. Marcos, "Aberrations of the human eye in visible and near infrared illumination," Optom. Vis. Sci. **80**, 26-35 (2003).
27. E. Fernandez, A. Unterhuber, P. Prieto, B. Hermann, W. Drexler, and P. Artal, "Ocular aberrations as a function of wavelength in the near infrared measured with a femtosecond laser," Opt. Express **13**, 400-409 (2005).
28. P. Perez-Merino, C. Dorronsoro, L. Llorente, S. Duran, I. Jimenez-Alfaro, and S. Marcos, "In vivo chromatic aberration in eyes implanted with intraocular lenses," Invest. Ophthalmol. Vis. Sci. **54**, 2654-2661 (2013).
29. L. N. Thibos, A. Bradley, and D. L. Still, "Interferometric measurement of visual acuity and the effect of ocular chromatic aberration," Applied optics **30**, 2079-2087 (1991).
30. E. Fernandez, A. Unterhuber, P. Prieto, B. Hermann, W. Drexler, and P. Artal, "Ocular aberrations as a function of wavelength in the near infrared measured with a femtosecond laser," Opt Express **13**, 400-409 (2005).
31. A. Guirao, J. Porter, D. R. Williams, and I. G. Cox, "Calculated impact of higher-order monochromatic aberrations on retinal image quality in a population of human eyes," J. Opt. Soc. Am. A **19**, 620-628 (2002).
32. D. R. Williams, D. H. Brainard, M. J. McMahon, and R. Navarro, "Double-pass and interferometric measures of the optical quality of the eye," J Opt Soc Am A Opt Image Sci Vis **11**, 3123-3135 (1994).
33. L. Sawides, P. de Gracia, C. Dorronsoro, M. A. Webster, and S. Marcos, "Vision is adapted to the natural level of blur present in the retinal image," PLoS ONE **6**, e27031 (2011).
34. P. de Gracia, S. Marcos, A. Mathur, and D. A. Atchison, "Contrast sensitivity benefit of adaptive optics correction of ocular aberrations," J. Vis **11**, 10 (2011).
35. Fianium, "Fianium. Supercontinuum sources" (Fianium Ltd, 2014), retrieved 2012, http://www.fianium.com/.
36. F. C. Delori, R. H. Webb, D. H. Sliney, and I. American National Standards, "Maximum permissible exposures for ocular safety (ANSI 2000), with emphasis on ophthalmic devices," J. Opt. Soc. Am. A **24**, 1250-1265 (2007).
37. "American National Standar for Safe Use of Lasers, ANSI Z.136.1-2007," (American National Standards Institute 2007).
38. J. I. Morgan, J. J. Hunter, B. Masella, R. Wolfe, D. C. Gray, W. H. Merigan, F. C. Delori, and D. R. Williams, "Light-induced retinal changes observed with high-resolution autofluorescence imaging of the retinal pigment epithelium," Invest. Ophthalmol. Vis. Sci. **49**, 3715-3729 (2008).
39. P. Artal, S. Marcos, R. Navarro, and D. R. Williams, "Odd aberrations and double-pass measurements of retinal image quality," J. Opt. Soc. Am. A **12**, 195-201 (1995).
40. S. Marcos, E. Moreno, and R. Navarro, "The depth-of-field of the human eye from objective and subjective measurements," Vision Res. **39**, 2039-2049 (1999).

41. L. N. Thibos, R. A. Applegate, J. T. Schwiegerling, R. Webb, V. S. T. M. V. science, and a. its, "Standards for reporting the optical aberrations of eyes," J. Refract. Surg. **18**, S652-660 (2002).
42. L. N. Thibos, X. Hong, A. Bradley, and R. A. Applegate, "Accuracy and precision of objective refraction from wavefront aberrations," J. Vis. **4**, 329-351 (2004).
43. M. Vinas, L. Sawides, P. de Gracia, and S. Marcos, "Perceptual Adaptation to the Correction of Natural Astigmatism," Plos One **7**(2012).
44. L. Sawides, S. Marcos, S. Ravikumar, L. Thibos, A. Bradley, and M. Webster, "Adaptation to astigmatic blur," J. Vis. **10**, 22 (2010).
45. L. Sawides, P. de Gracia, C. Dorronsoro, M. Webster, and S. Marcos, "Adapting to blur produced by ocular high-order aberrations," J. Vis. **11**(2011).
46. D. R. Williams, D. H. Brainard, M. J. McMahon, and R. Navarro, "Double-pass and interferometric measures of the optical quality of the eye," J. Opt. Soc. Am. A **11**, 3123-3135 (1994).
47. T. O. Salmon, L. N. Thibos, and A. Bradley, "Comparison of the eye's wave-front aberration measured psychophysically and with the Shack-Hartmann wave-front sensor," J Opt Soc Am A Opt Image Sci Vis **15**, 2457-2465 (1998).
48. S. Marcos and S. A. Burns, "Cone spacing and waveguide properties from cone directionality measurements," J. Opt. Soc. Am. A **16**, 995-1004 (1999).
49. N. Lopez-Gil and P. Artal, "Comparison of double-pass estimates of the retinal-image quality obtained with green and near-infrared light," J. Opt. Soc. Am. A **14**, 961-971 (1997).
50. A. M. Bagci, M. Shahidi, R. Ansari, M. Blair, N. P. Blair, and R. Zelkha, "Thickness profiles of retinal layers by optical coherence tomography image segmentation," Am. J. Ophthalmol. **146**, 679-687 (2008).
51. M. Karampelas, D. A. Sim, P. A. Keane, V. P. Papastefanou, S. R. Sadda, A. Tufail, and J. Dowler, "Evaluation of retinal pigment epithelium-Bruch's membrane complex thickness in dry age-related macular degeneration using optical coherence tomography," Br. J. Ophthalmol. **97**, 1256-1261 (2013).
52. V. Manjunath, M. Taha, J. G. Fujimoto, and J. S. Duker, "Choroidal thickness in normal eyes measured using Cirrus HD optical coherence tomography," Am. J. Ophthalmol. **150**, 325-329 e321 (2010).
53. F. C. Delori and K. P. Pflibsen, "Spectral reflectance of the human ocular fundus," Appl. Opt. **28**, 1061-1077 (1989).
54. S. Ravikumar, L. N. Thibos, and A. Bradley, "Calculation of retinal image quality for polychromatic light," J. Opt. Soc. Am. A **25**, 2395-2407 (2008).
55. A. E. Elsner, S. A. Burns, J. J. Weiter, and F. C. Delori, "Infrared imaging of sub-retinal structures in the human ocular fundus," Vision Res. **36**, 191-205 (1996).
56. E. Fernandez and W. Drexler, "Influence of ocular chromatic aberration and pupil size on transverse resolution in ophthalmic adaptive optics optical coherence tomography," Opt. Express **13**, 8184-8197 (2005).
57. K. Grieve, P. Tiruveedhula, Y. Zhang, and A. Roorda, "Multi-wavelength imaging with the adaptive optics scanning laser Ophthalmoscope," Opt. Express **14**, 12230-12242 (2006).

1. Introduction

The retinal image quality is degraded by the presence of monochromatic and polychromatic aberrations in the ocular optics. However, ocular aberrations are measured using wavefront sensors with monochromatic, generally infrared, light. Nevertheless, the visual world is polychromatic and the study of the impact of retinal image quality on vision should consider the aberrations in the visible light, as well as the effect of chromatic aberrations.

Chromatic effects in the eye arise from the wavelength-dependence on the refractive index of the ocular media (chromatic dispersion), affecting diffraction, scattering and aberrations [1-3]. In particular, chromatic dispersion causes short wavelengths to focus in front of long wavelengths, producing a chromatic difference of focus between the shorter and longer wavelengths, known as Longitudinal or axial Chromatic Aberration (LCA) [4]. In addition, optical irregularities, misalignments between the ocular components and the off-axis position of the fovea result in a transversal shift of focus for different wavelengths, known as Transverse Chromatic Aberration (TCA) [5-8]. In polychromatic light, the retinal image quality is

affected by interactions between monochromatic and chromatic aberrations. It has been suggested that monochromatic aberrations play a protective role against chromatic aberrations [9], which may explain why achromatizing lenses [10, 11] aimed at correcting LCA in the eye do not noticeably improve visual performance, unless both chromatic and monochromatic aberrations are corrected [12].

Since the demonstration by Young [13] and Helmholtz [14] of the variation of power of the human eye across the visible spectrum, LCA has been measured extensively. It is fairly accepted that LCA is rather constant across the population, almost invariant in small and moderate angles across the visual field [15], and fairly constant with age [16, 17], although some studies have reported an age-dependent decrease of LCA [18, 19].

LCA has been measured using different psychophysical techniques (i.e. stigmatiscope [4, 20], Badal optometer [21], Vernier alignment [17], or the spatially resolved refractometry [22]) and across different spectral ranges [14, 23]. Reports of psychophysical LCA span from 3.20 D in a 365-750 nm range [20] to 1.33 D in a 450-650 nm range [22]. Psychophysical data of LCA have been used to derive an average Cornu's expression for the dependence of the index of refraction with wavelength (in the 400-700 nm range). This expression is used in chromatic eye models, i.e. the Indiana chromatic reduced eye model, to predict the chromatic focus shift between two given wavelengths [24].

LCA has also been measured objectively by means of reflectometric techniques, such as double-pass retinal images of a slit [25] or of a point source [15] at different wavelengths. Reports of reflectometric LCA span from 1.40 D (460-700 nm) [25] to 1.00 D (458-632 nm) [15]. More recently, chromatic difference of focus between two wavelengths has been obtained from objective wavefront sensing (Hartmann-Shack and Laser Ray tracing) with a value of 0.72 D (532-787 nm) [26] and 0.40 D in the NIR (700-900 nm) [10, 27]. Only recently, LCA has been measured objectively by means of reflectometric techniques in pseudophakic eyes, with great implications in new designs of intraocular lenses (IOLs). Perez-Merino et al. (2013) have reported the chromatic difference of focus in two groups of pseudophakic eyes implanted with IOLs of different materials, and found statistical differences, consistent with the Abbe number of the IOL materials (0.46 and 0.75 D, respectively), in the 532-787 nm range [28].

Despite the differences in the chromatic ranges and studies, there seems to be a consistent discrepancy between psychophysical and double-pass-based measurements of LCA, with the objective values underestimating the psychophysical values. These differences between objective and psychophysical LCA were observed in measurements on the same subjects where the discrepancies mostly occurred in the shorter wavelength range

[25]. A later study compared the objective best focus (from double-pass aerial images) with the subjective best focus of a point source, and showed that objective data were slightly lower that subjective at the fovea and for 6-mm pupil [15]. The lower estimates of LCA from reflectometric double-pass techniques [16, 27] have been hypothesized to arise from the wavelength-dependence of the reflectivity of the different retinal layers [12]. Additionally some authors have speculated that the presence of monochromatic aberrations may affect differently the psychophysical and reflectometric measurements of chromatic aberration [24, 29]. The differences across studies in the measurement techniques and spectral ranges pose uncertainty on the actual magnitude of the differences between psychophysical and reflectometric LCA, and limits the assessment of the different hypotheses.

In this study, we present LCA from psychophysical and reflectometric methods performed on the same group of subjects using the same instrument in a wide spectral range. The psychophysical LCA was obtained in the visible range (488-700 nm) and the LCA from reflectometric techniques was obtained both in the visible (488-700 nm) and near-infrared ranges (700-900 nm). Reflectometric techniques included both through-focus double-pass retinal images and wavefront sensing. All measurements were obtained using a new custom-developed Adaptive Optics (AO) system, provided with a supercontinuum laser source, a psychophysical channel, a double-pass imaging channel, and a Hartman-Shack wavefront sensor. An electromagnetic deformable mirror allows measurements under natural and corrected monochromatic aberrations.

The study therefore provides, to our knowledge, the first evaluation of the change of high order aberrations with wavelength using objective aberration in the visible spectrum. A previous study [22] reporting high order aberrations across visible light used the spatially resolved refractometer, where aberrations were measured through a psychophysical (non-reflectometric) technique. A previous study [30] using Hartmann-Shack aberrometry reported non-significant changes in the high order aberrations with wavelength in the 700-900 nm. Also, to our knowledge, this is the first time where subjective and objective focus (estimated from Hartman-Shack wavefront measurements) is compared at different wavelengths in visible light. Normally the studies [31, 32] relating subjective and objective best focus have been performed with white and black targets stimulus (for subjective focus) and retinal image quality metrics based on monochromatic aberrations (generally infrared) for estimation of objective best focus, assuming a constant shift produced by LCA. Recent studies have shown that in fact the best focus setting may be substantially biased by blur adaptation, and the perceived best focus not necessarily well predicted by optical model, thus justifying the interest of

performing both psychophysical and objective experiments at different wavelengths [33]. Finally, the availability of an adaptive optics system in the same set-up offers a unique opportunity to test a hypothesis stated by previous authors as a potential cause of discrepancy between subjective and reflectometric techniques [24, 29]. If high order aberrations are independent of wavelength (as confirmed in this study) the lack of influence of the high order aberrations on the LCA could have been ruled out, assuming that best focus can be fully predicted by optical models. However, as psychophysical functions are not always well predicted by optical theory [34], performance of the psychophysical testing in the absence of high order aberrations (as corrected by Adaptive Optics) allows to ultimately testing the hypothesis.

2. Materials and methods

Longitudinal Chromatic Aberration (LCA) was obtained from reflectometric and psychophysical measurements of best focus at 15 different wavelengths on 5 eyes from 5 normal subjects. A custom-developed polychromatic Adaptive Optics (AO) system was used for these measurements.

2.1 Polychromatic Adaptive Optics setup

Figure 1 shows a schematic diagram of the polychromatic custom-developed AO system, specifically developed for this study. The instrument allowed correction of the aberrations of the subject, while performing psychophysical settings of best focus, acquisition of double-pass retinal images or wavefront aberration measurements at different wavelengths.

A supercontinuum laser source (SCLS, SC400 femtopower 1060 supercontinuum laser, Fianium Ltd, United Kingdom) [35] which delivers a supercontinuum spectrum, spanning from below 450 nm to beyond 1100 nm (in our system configuration), was used as the light source (4.16 W power, 40 MHz fixed repetition rate, 400 fs pulse duration, and 50 nJ maximum pulse energy). A dual acousto-optic tunable filter (AOTF) module (Gooch & Housego, United Kingdom) coupled to the SCLS and operated by RF drivers is used to automatically select the desired wavelengths: 450, 488, 500, 532, 555, 570, 633 & 700 nm in the VIS-Channel and 730, 780, 810, 827, 850, 880, 950 & 1020 nm in the NEAR-Channel, with an average spectral bandwidth of 5 nm (2-4 nm (VIS); 3-6 nm (NIR)). The output is a collimated beam coupled to two independent multimode fibers. Both the main source and the RF drivers are software-controlled. The laser power measured at the corneal plane ranged between 0.5 and 50 μW, which was at least one order of magnitude below the ANSI standards safety limits at all tested wavelengths [36-38].

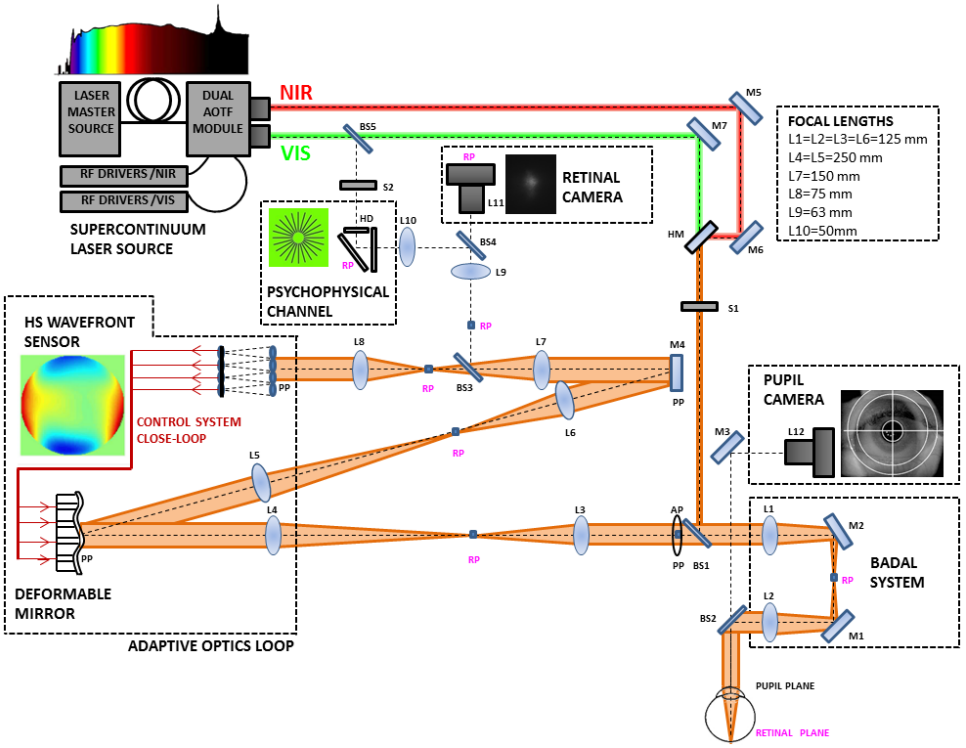

Fig. 1. Custom-made polychromatic adaptive-optics setup.

The main components of the AO-system are: (1) a Hartmann-Shack wavefront sensor, which measures the ocular aberrations; (2) an electromagnetic deformable mirror, which corrects aberrations; (3) a double-pass retinal imaging system, which captures retinal aerial images; (4) a psychophysical channel, which allows projection of psychophysical stimuli; (5) a Badal system which corrects for defocus in channels 1, 3 and 4; and (6) a pupil monitoring channel.

Illumination coming from the two independent fiber-channels of the SCLS enters the system collinearly by means of a hot mirror (HM). A Badal system (consisting of mirrors M1 & M2, and lenses L1 & L2), mounted on a motorized system, is used to compensate for the spherical error of the eye. The Badal system can be controlled automatically or with a keyboard operated by the subject to adjust his/her subjective best focus.

The Hartmann-Shack wavefront sensor consists of a microlens array of 40x32 microlenses and 3.6-mm effective diameter, centered at 1062 nm (HASO 32 OEM, Imagine Eyes, France). The 2-mm diameter beam entering the eye is slightly (1 mm) decentered with respect to the pupil center to avoid a corneal reflex in the Hartmann-Shack images. The electromagnetic deformable mirror (52 actuators, a 15-mm effective diameter and a 50-µm stroke; MIRAO, Imagine Eyes, France) is used to correct the aberrations of the system and the subjects' eyes. Light reflected

off the retina passes the Badal system, the deformable mirror, and is focused on the CCD camera of the Hartmann-Shack wavefront sensor by the microlens array. The deformable mirror is conjugated to the pupil by a pair of relay lenses (L3 & L4 with 125-mm and 250-mm focal length respectively) with x2 magnification factor from the pupil to the mirror. The microlens array is conjugated to the pupil by 2 pairs of relay lenses (L5 & L6, 250-mm and 125-mm focal lengths respectively; and L7 & L8, 150-mm and 75-mm focal lengths) with x0.5 magnification factor from the pupil to the microlens array. A 6-mm artificial pupil (AP), placed in conjugate pupil plane, ensures constant pupil diameter in the measurements.

The double-pass retinal imaging channel is inserted by means of a 70/30 beam splitter. Images of the beam spot are projected on a scientific-grade CCD camera (Retiga 1300, CCD Digital Camera, 12-bit, Monochrome; QImaging, Canada; 6.7x6.7 μm pixel size, 1024x1280 pixels) by means of a collimating lens (L9, 63-mm focal length) and a camera lens (L11, 135-mm focal length). This channel acts as a "one-and-a half pass", with the aerial image being the autocorrelation [39] of the image of the laser spot with a 2-mm entry beam and that with a 1-mm exit beam.

The psychophysical channel contains a slide with a sunburst chart (with spatial frequencies ranging from 3.5 to 150 cycles/deg) located in a conjugated retinal plane (Fig. 1), The visual stimulus subtends 1.62 degrees on the retina, and is monochromatically back-illuminated with light coming from the SCLS. Two automatized shutters allow simultaneous illumination of the eye (S1) and the stimulus (S2). A holographic diffuser (HD) placed in the beam path breaks the coherence of the laser providing a uniform illumination of the stimulus. The luminance of the stimulus was 20-25 cd/m^2 across the spectral range tested psychophysically (450-700 nm), therefore in the photopic region at all wavelengths.

The natural pupil monitoring system consists of a camera (DCC1545M, High Resolution USB2.0 CMOS Camera, Thorlabs GmbH, Germany) conjugated with the eye's pupil by means of an objective lens (L12, 105-mm focal length). It is inserted in the system using a plate beam-splitter, and is collinear with the optical axis of the imaging channel. Subjects are aligned to the system (using an x-y-z stage moving a bite bar) with the line of sight as a reference while viewing the natural pupil on the monitor.

2.2 System control and calibration

All optoelectronic elements of the system (SCLS main source, Badal system, retinal image camera, pupil camera, Hartmann-Shack and deformable mirror) are automatically controlled and synchronized using custom-built software programmed in Visual C++ and C# (Microsoft, United States). The dual AOTF system is controlled with the software provided by the manufacturer. The AO system custom-developed routines

use the Software Development Kit from the manufacturer (centroiding detection, wave aberration polynomial fitting and closed-loop operation).

The monochromatic aberrations of the system were measured and corrected by AO closed-loop correction using an artificial eye (consisting of a 50.8-mm focal length achromatic doublet lens and a rotating diffuser as an artificial retina). A modal control was used. The state of the mirror that compensates for the system's aberrations is saved and applied when measurements are performed under natural aberrations. The wave aberration of the artificial eye is measured with the wavefront sensor and kept as a reference file (tilt and defocus are measured but kept free). To correct the aberrations, the residual wavefront is continuously measured and command controls are sent to the deformable mirror in a closed-loop operation. In measurements performed under a static correction, the deformable mirror state that compensates the aberrations is used during each test, and updated between runs. Discrepancies in the measured aberrations were typically less than 4% with respect to nominal values in artificial eyes with known aberrations. A correction of 95% of the RMS wavefront error is typically achieved

The LCA of the setup was calibrated by measuring the system's aberrations, and estimating the chromatic difference of focus from the defocus Zernike coefficient (C_2^0) at all wavelengths (450-1020 nm). For calibration, the beam coming from the SCLS was directed (using mirrors but not lenses) to a concave mirror at far distance (1 m from the pupil plane of the system) that created a virtual point source, the same at all wavelengths. The light reflected from the concave mirror traversed the system in one-pass and was collected by the Hartman-Shack wavefront sensor, while the electromagnetic deformable mirror corrected for the aberrations of the system. These measurements were compared with those obtained using the artificial eye in place of the patient's eye. Both methods provided similar setup's LCA values (within 4%). In the visible range, (450-700 nm) the measured setup's LCA was negligible ~0.00 D (as expected, as all lenses in the system are achromatic doublets for visible light), while in the (700-1020 nm) it was 0.29 D.

2.3 Subjects

Five young subjects (28.60±1.89 years) participated in the experiment. Spherical errors ranged between 0 and -4.50 D (-1.15±0.95 D), and astigmatism was ≤ -0.5 D in all cases. All experiments were conducted under cycloplegia (Tropicamide 1%, 2 drops 30 minutes prior to the beginning of the study, and 1 drop every 1 hour). All participants were acquainted with the nature and possible consequences of the study and provided written informed consent. All protocols met the tenets of the

Declaration of Helsinki and had been previously approved by the Spanish National Research Council (CSIC) Ethical Committee.

2.4 Experiments

Subjective and objective best focus was obtained for each of the tested wavelengths. All measurements were performed using 6-mm pupil diameters, both for natural aberrations (i.e. correcting the aberrations of the optical system only) and AO-corrected aberrations. The best subjective focus was initially searched with the stimulus back-illuminated at reference wavelength of 555 nm. All settings are referred to the best subjective focus at this wavelength obtained with either natural or AO-corrected aberrations. The state of the mirror that compensates for the ocular aberrations of each eye was found in a closed-loop operation at 827 nm (NIR), and applied in measurements at all wavelengths, as a preliminary experiment showed no benefit of changing the aberration-correcting state of the mirror (measured at each wavelength) for measurements at that given wavelength. For example, the state of the mirror that corrected for the aberrations of the system and the subject at 555 nm (visible light) in a subject resulted in 0.0391 μm RMS residual aberrations. The same state of the mirror applied at 827 nm resulted in 0.0427 μm RMS.

Aberrations were monitored throughout the experiment to ensure that each state was performed under the desired state of aberration corrections. Experiments were performed first under natural aberrations and then under AO-correction. The following measurements were performed, in this order:

Experiment 1. Psychophysical best focus. Subjects adjusted their best subjective focus using the Badal system while looking at the stimulus back-illuminated with a series of wavelengths in visible light: 450, 488, 500, 532, 555, 570, 633 & 700 nm. Subjects were instructed to use the keyboard to move the Badal system to find the position where the stimulus appeared sharp. Subjects performed first a trial run to become familiar with the test. Focus search was repeated 3 times for each wavelength.

Experiment 2. Through-focus double pass retinal aerial images at different wavelengths. Retinal aerial images were obtained while the Badal system was moved from -1.50 D to +1.50 D in 0.25-D steps (around the best subjective focus at 555 nm). These measurements were obtained both in visible light (488, 500, 532, 555, 570, 633 & 700 nm) and near IR light (730, 780, 810, 827, 850, 880 & 950 nm).

Experiment 3. Hartmann-Shack wave aberrations at different wavelengths. Wave aberrations were measured in visible light (488, 500, 532, 555, 570, 633 & 700 nm) and near IR light (730, 780, 810, 827, 850, 880 & 950 nm), while the Badal system corrected the subject's subjective defocus at 555 nm.

Experiments 4, 5 and 6, were identical to Experiments 1, 2, and 3, but under AO-correction. Psychophysical measurements in *Experiment 4* were performed for the same wavelengths than in Experiment 1. Experiments 5 and 6 were performed for 488, 500, 555 & 700 nm in visible light and 730, 880 & 950 nm in near IR light, to avoid the fatigue of the subjects. The reference for best focus at 555 nm was obtained subjectively first under natural aberrations for Experiments 1, 2 and 3, and under AO-correction for Experiments 4, 5, and 6.

2.5 Data analysis

The best subjective foci at each wavelength from Experiment 1 were directly obtained from the automatic readings of the Badal system. The best foci from Experiment 2 were obtained by analysis of the through-focus retinal aerial image series for each wavelength [40]. The best focus image from the series was obtained from the focus position corresponding to the image with minimum spread (lower width at half-height).

The wave aberrations measured in Experiment 3 were fitted by 7th order Zernike polynomials. The OSA convention was used for ordering and normalization of Zernike coefficients [41]. For each wavelength, defocus in diopters, *D,* was obtained from the 2nd order Zernike defocus coefficient (C_2^0) in microns, using Eq. (1).

$$\mathrm{D} = -4.C_2^0.\sqrt{3}/\mathrm{r}^2 \qquad \text{[Eq. (1)]},$$

where C_2^0 is the Zernike defocus and *r* is the pupil diameter [42].

In an alternative analysis, best focus was obtained from through-focus Strehl Ratio (SR) simulations calculated from the measured wave aberrations, as the maximum of the Point Spread Function (PSF) relative to the diffraction-limited-PSF, for 6-mm pupils and the corresponding wavelength. The best focus was obtained from the maximum of the peak of the calculated through-focus SR curves for each measured wavelength. A control simulation showed that the best focus obtained from the retinal image quality metrics (minimum spread and Strehl ratio, as well as volume under the MTF in the spatial frequency range of the target stimulus), was within 0.15 D, on average. Chromatic difference of focus curves were obtained from the data of best focus of each experiment. The LCA was obtained from the polynomial fitting of those curves. The curves are shifted in the vertical axis such that they cross zero at 555 nm (the reference wavelength). For the psychophysical data, LCA was computed for the visible range only. For the reflectometric experiments, LCA was computed for visible (488-700 nm, VIS), near IR (700-950 nm, NIR) and total (488-950 nm, TOTAL) ranges. Focus setting reproducibility was obtained from measurements of best focus for one subject and all wavelengths, based on 5 focus settings both for natural and AO-corrected aberrations. Variability in

focus setting was < 0.05 D for all wavelengths, except in wavelengths at the end of the spectral ranges (450 and 700 nm), where the variability was 0.1 D.

Statistical analysis was performed with SPSS software (IBM, United States) to test differences in the estimated LCA across experiments. A non-parametric paired samples t-test with *post hoc* Wilcoxon Signed Ranks test was performed to analyze specific differences between conditions.

3. Results

LCA was obtained from measurements of best focus at different wavelengths from psychophysical (Experiment 1/4) and reflectometric (Experiments 2-3/5-6) experiments, with natural and corrected aberrations.

3.1. Wave aberration measurement and correction at different wavelengths

Figure 2 shows wave aberration maps for astigmatism and HOA (Fig.2 (a)) and their corresponding RMS (Fig. 2 (b)) for selected measured wavelengths in one subject, with natural aberrations and AO-correction. Wave aberrations maps are similar, with no systematic variation, across wavelengths. The RMS standard deviation across wavelengths was 0.04 µm for natural aberrations and 0.01 µm for AO-correction, averaged across subjects. Residual RMS upon AO-correction was lower than 0.05 µm.

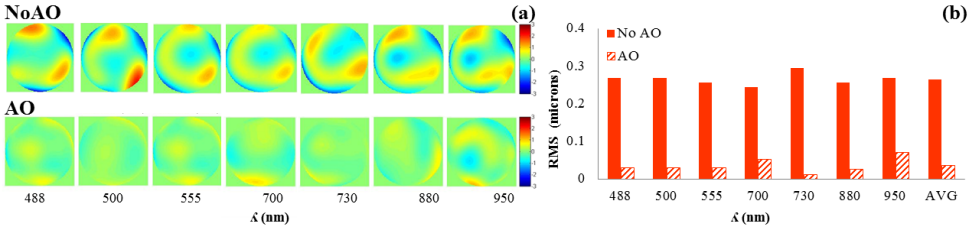

Fig. 2. (a) Wave aberrations map for astigmatism and HOA for selected wavelengths in Subject #3 with natural aberrations (upper row) and AO-correction (lower row). (b) Corresponding RMS. Data are for 6-mm pupils.

3.2. Through-focus image quality at different wavelengths (measurements and simulations)

Through-focus double-pass retinal images (Experiment 2/5) and through-focus SR (calculated from wave aberrations, Experiment 3/6) was used to estimate best focus for each wavelength. Figure 3 shows examples of through-focus experimental aerial images (Fig. 3(a)), and simulated through-focus Point Spread Functions (PSF), with natural aberrations (Fig. 3(b)), and with AO-correction (Fig. 3(c)); best focus obtained from series of double-pass images, with natural aberrations and AO correction (Fig. 3(d)) and best focus obtained from through-focus SR calculations for natural aberrations (Fig. 3(e)) and AO-correction (Fig. 3(f)).

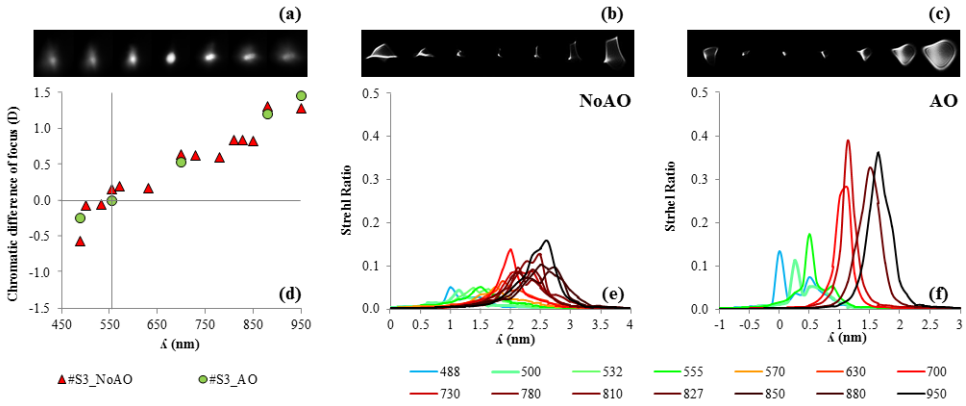

Fig. 3. (a) Example of experimental through-focus double-pass retinal images for subject #S1 at 555 nm with natural aberrations. (b) Example of simulated through-focus PSF at 555 nm for #S2 under natural aberrations, and (c) under AO-correction. (d) Chromatic difference of focus obtained from series of double-pass images at all measured wavelengths for subject #S3, with natural aberrations (Red triangles), and AO-correction (Green circles). (e) Through-focus Strehl Ratio (SR) calculated from measured wave aberrations at each wavelength for subject #S2 under natural aberrations, and (f) under AO-correction.

3.3 Chromatic difference of focus from psychophysical and reflectometric techniques

Figure 4 shows the measured chromatic difference of focus from psychophysical measurements [Experiment 1, Fig. 4(a)], through focus retinal images [Experiment 2, Fig. 4(b)] and defocus Zernike coefficient [Experiment 3, Fig. 4(c)] for all 5 subjects and all measured wavelengths, under natural aberrations, upper row, Figs. 4(a)-(c), and AO-correction, Figs. 4(d)-(f).

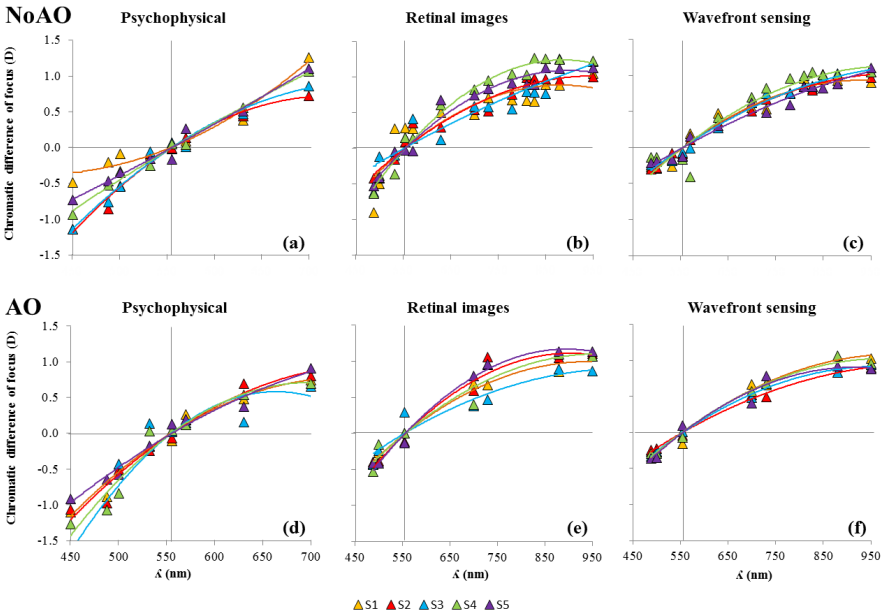

Fig. 4. Chromatic difference of focus (a) from subjective best focus; (b) from series of double-pass retinal images; (c) from the defocus Zernike coefficient of measured wave aberrations, at different wavelengths. (a-c) Under natural aberrations. (d-e) As in (a-c), but with AO-correction. Data are referred to the best focus at 555 nm for each technique, set as zero defocus.

Figure 5 compares chromatic difference of focus curves across the different techniques, averaged across subjects, for natural aberrations [Fig. 5(a)] and AO-correction [Fig. 5(b)]. The difference between the curve fitting the psychophysical data and that fitting the reflectometric data (0.107 RMS difference for double-pass and 0.769 RMS for wavefront sensing, for natural aberrations and 0.014 RMS difference double-pass and 0.307 RMS for wavefront sensing, for AO-correction) is significantly higher (paired-samples t-test, p=0.004) than the difference between the curves fitting either reflectometric data (0.044 RMS difference for natural aberrations and 0.057 RMS for AO-correction). There is also great similarity between data obtained under natural aberrations and AO-correction (0.3078, 0.0071, and 0.0032 RMS difference for averaged psychophysical data, wavefront sensing data, and double-pass).

Table 1. Chromatic difference of focus

	Green-Blue/555-488 nm		Green-Red/555-700 nm	
	NoAO	**AO**	**NoAO**	**AO**
Psychophysical	0.53 D	0.75 D	0.99 D	0.74 D
Retinal images	0.35 D	0.41 D	0.59 D	0.65 D
Wavefront sensing	0.33 D	0.33 D	0.55 D	0.55 D
Strehl Ratio	0.32 D	0.32 D	0.55 D	0.54 D

The chromatic difference of focus between green and blue wavelengths was smaller than between and green and red wavelengths in all techniques, although in both ends the chromatic difference of focus was larger for psychophysical than for reflectometric techniques. Table 1 shows the chromatic difference of focus for green-blue and green-red for all techniques, both under natural aberrations and AO-correction.

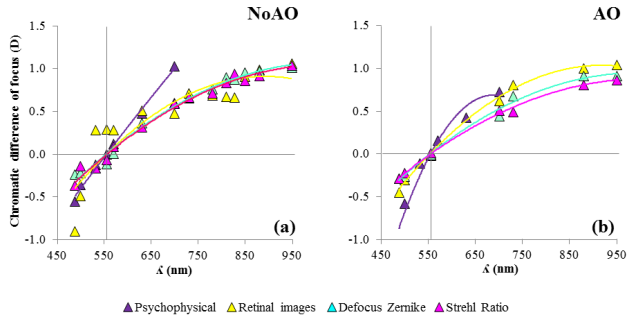

Fig. 5. (a) Chromatic difference of focus for all 4 techniques: psychophysical, purple; retinal images, yellow; wavefront sensing/defocus Zernike term, green; wavefront sensing/Strehl Ratio, magenta. Data are averaged across subjects; (a) from measurements with natural aberrations. (b) As in (a) butfrom measurements with AO-correction of natural aberrations. Data are referred to 555 nm by shifting the polynomial regressions of the measured data.

3.4. LCA: differences across techniques

Figure 6 shows LCA in the visible spectral range common to all techniques (488-700 nm); and LCA in the near IR spectral range (700-950 nm) and total spectral range (450-950 nm) from reflectometric techniques, both with natural aberrations and with AO-correction. The LCA for the largest available spectral range in the visible (450-700 nm was on average 1.84±0.05 D from psychophysical data. The LCA in the 488-700 nm range was 1.52 D from psychophysics, and 0.95 D and 0.88 D from retinal images and wavefront sensing reflectometric techniques, under natural aberrations. The LCA for the total spectral range was 1.41 D and 1.34 D from for retinal images and wavefront sensing, respectively.

The LCA from psychophysical experiments is statistically significantly higher (paired-samples t-test, $p<0.01$) than that from the reflectometric techniques. There are no statistically significant differences in LCA for neither the visible, NIR or total spectral range from all reflectometric techniques (paired-samples t-test, $p=0.42$; $p=0.95$ and $p=0.49$, respectively). Intersubject variability is small for all techniques: psychophysical, ±0.04 D for VIS, retinal images, ±0.07 D, and wavefront sensing, ±0.06 D for the total spectral range, in the presence of natural aberrations.

3.5 LCA: impact of the presence of high order aberrations

Correction of the eye's natural aberrations produces a shift of the best focus, due to interactions between defocus and spherical aberration (and likely other HOA). The average difference in this shift (across subjects and wavelengths) was 0.35±0.12 D for psychophysical measurements, 0.21±0.10 D for double-pass, 0.18±0.05 D for the defocus Zernike coefficient, and 0.27±0.04 D from simulated SR. In all subjects this shift was constant across wavelengths. This result suggests that the presence of aberrations play a negligible role in the LCA, regardless the technique.

Figure 6 shows the LCA obtained from each technique, under natural and AO-corrected aberrations. In general, the presence of natural aberrations does not change LCA significantly, in neither psychophysical or reflectometric techniques, except for in the double-pass LCA in the visible range (paired-samples t-test, $p<0.02$).

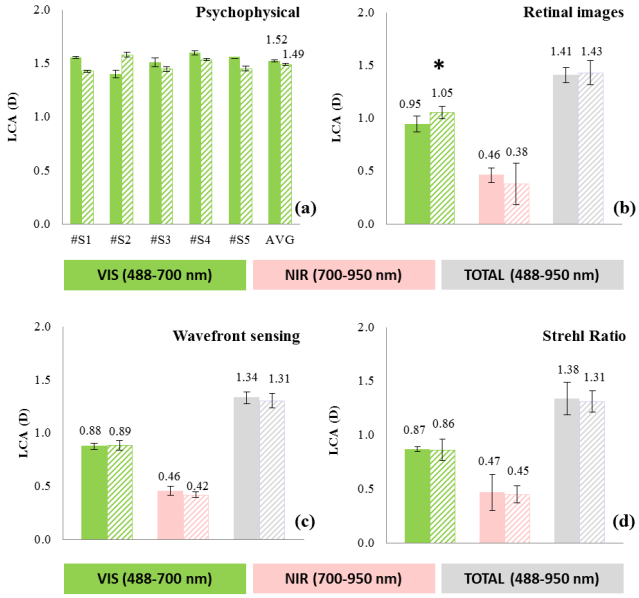

Fig. 6. LCA averaged across subjects from (a) subjective best focus, (b) retinal images, (c) wavefront sensing and (d) Strehl Ratio for the different spectral ranges: VIS, NIR and TOTAL. Solid bars indicate Natural aberrations, and dashed bars indicate AO-correction; (*) stands for statistically significant differences ($p = 0.02$) Error bars stand for standard deviations of repeated measurements for subjective LCA and standard deviation across subjects for the other techniques.

4. Discussion

We have shown that: (1) ocular LCA shows low intersubject variability; (2) the LCA from a psychophysical method is significantly higher (by 0.50 D in the 488-700 nm range) than the LCA measured using reflectometric techniques, and (3) the LCA (from either psychophysical or reflectometric techniques) is independent of the presence of HOA.

The observed differences between the psychophysical and reflectometric LCA may arise, as previously proposed, from the fact that the retinal reflection may not occur at the plane at which the retinal image must be focused to give the best subjective image at all wavelengths.

4.1 Comparison of LCA with previous studies

Our study provides estimates of the LCA measured across a wider spectral range in the visible and IR than that of previous studies. Figure 7 shows the chromatic difference of focus found in the current study (psychophysical, purple; reflectometric, yellow), in comparison with the predictions of the Indiana chromatic reduced eye model (black) [24] and the chromatic difference of focus reported in previous studies for different spectral ranges, using psychophysical (blue) and reflectometric (orange) methods. In general, our results are in good agreement with previous studies using psychophysical and reflectometric techniques. The Indiana chromatic reduced eye model, built using experimental data [26], predicts a chromatic focus shift of 1.00 D for VIS, 0.44 D for NIR, and 1.45 D for TOTAL. The chromatic eye model seems to fit well the psychophysical data for shorter wavelengths and the reflectometric data for longer wavelengths. There is a general good agreement with data in shorter ranges from previous studies, both psychophysical and reflectometric.

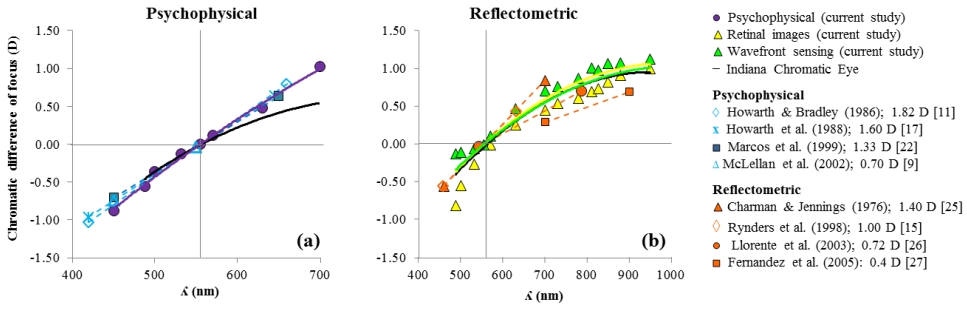

Fig. 7. (a) Chromatic difference of focus from the psychophysical measurements of the current study (purple), the predictions from the Indiana chromatic reduced eye model (black), and psychophysical data in the literature (blue) in the visible range. (b) Chromatic difference of focus from the reflectometric measurements (yellow, from retinal images; green, from wavefront sensing) of the current study, the predictions from the Indiana chromatic reduced eye model (black), and reflectometric data in the literature (orange) in the visible and NIR range. The measured chromatic range differed across studies, and it is indicated by the symbols in the end of the regression curves. The numbers indicate the corresponding literature reference (see legend). Data are referred to zero defocus at 555 nm.

4.2 Impact of natural aberrations: subjective vs. subjective focus

The presence of HOA shifts the position of best focus from the best focus in absence of aberrations. Although neural adaptation to astigmatism or HOA may alter the perceived best focus position with respect to that predicted solely by optics [43-45], several studies indicate that subjective

refraction can, in general, be well predicted from objective measurements (wave aberrations or double-pass), particularly when retinal image based metrics are used [8, 22, 31]. Similarly, retinal image quality metrics predict well the best focus shift between natural aberrations and AO-correction [40]. Here, we have shown that the shift in best focus caused by the presence of natural aberrations is constant across wavelengths. This indicates that, while the absolute best focus is affected by the presence of aberrations, this occurs at all wavelengths equally, and therefore LCA remains unaffected by the presence of aberrations (i.e. measurements with a larger or smaller pupil, etc), ruling out the potential role of HOA in the differences between psychophysical and reflectometric LCA suggested by previous authors [24, 29, 46, 47].

4.3 Psychophysical vs reflectometric LCA: effect of retinal reflection

It has been suggested that most of the light contributing to the core of double-pass aerial images likely comes from the light captured and guided back from the photoreceptors [25, 41]. The halo appearing in the double pass images is likely produced by effects other than aberrations, such as retinal stray light scattered at the choroid [46]. Retinal scattering increases for longer wavelengths due to their deeper penetration within the retina and the choroid [26]. The relative contribution of the directional component coming from the photoreceptors, the diffuse component coming from other retinal layers, choroid and optically turbid media, and a specular component, coming from smooth boundaries of optical media (such as the inner limiting membrane or corneal surface), is wavelength-dependent [15]. Photoreceptor alignment reflectometry demonstrates a high directional component in green light, which is highly reduced in IR [48]. The directional component will be highly concentrated around the central peak of the aerial image, whereas diffuse or (defocused) specular components will yield little contribution to the peak, and lead to potential differences in the plane identified as in focus. Some studies have reported negligible differences between psychophysical and reflectometric focus, concluding that reflection contributing to the central core of the point-spread function occurred within the photoreceptor layer [26, 46, 49]. However, while this may be true for wavelengths close to the peak of retinal sensitivity (green-red light) it not may be the case for shorter or longer wavelengths.

Assuming that best focus from psychophysical and reflectometric techniques matches at 555 nm, the average data in Figure 5 shows that the deviations occur both at the short and long range of the spectrum. At 488 nm the average difference between psychophysical and reflectometric best focus is 0.25 D, which, from a schematic reduced eye model, corresponds to blue light being reflected 128 μm anteriorly from the photoreceptors inner segments, approximately in the retinal nerve fiber layer in the retina.

At 700 nm, the shift is 0.54 D, suggesting that the reflection occurs 370 μm behind the photoreceptors, in the choroid [50-52]. This fact is interesting since in red light the contribution of the choroidal reflections is large compared with that of reflections originating in the inner layers of the retina [53], and might explain the higher shift in red than in blue light.

This non-symmetric contribution of red and blue light to chromatic defocus should be considered when calculating the retinal image quality for polychromatic light [54]. An accurate knowledge of the ocular LCA is useful for identifying the focus shifts necessary to convert aberrometric (and refractometric) measurements typically obtained in the IR into visible wavelengths. Knowledge of chromatic aberration is also important for *in vivo* retinal imaging, especially when pursuing multi-wavelength imaging [55] with conventional fundus cameras, Scanning Laser Ophthalmoscopy (SLO), or Optical Coherence Tomography (OCT) [56]. In addition, in multi-wavelength Adaptive Optics SLO, correcting for the eye's chromatic aberrations is necessary in applications that require imaging simultaneously in identical depths with two wavelengths [57]. A better understanding of the interactions between chromatic and polychromatic aberrations is also important in the study of the limits to spatial vision, and more practically for the material selection and design of new intraocular lenses.

Acknowledgments

This research has received funding from the European Research Council under the European Union's Seventh Framework Program (FP/2007-2013) / ERC Grant Agreement. [ERC-2011-AdC 294099]. This study was also supported by Spanish Government grant FIS2011-25637 to SM, CSIC JAE-Pre programs & MICINN FPU Predoctoral Fellowship to MV, and CSIC JAE-Tec program to DC.